Thermal Properties and Characterization of n-Decanol-Capric Acid/Expanded Graphite/Boron Nitride for Thermal Energy Storage

Tongqiang LIANG [1], Piaopiao HUANG [2]*, Yanghua CHEN [3], Junkang WU [1]

[1] *College of Intelligent Manufacturing Engineering, JiangXi Institute of Applied Science and Technology, Nanchang 330100, China*
[2] *CRRC Zhuzhou Electric Locomotive Research Institute Co., Ltd., Zhuzhou 412000, China*
[3] *College of Mechatronics Engineering, Nanchang University, Nanchang 330031, China*

http://doi.org/10.5755/j02.ms.33351

Received 7 February 2023; accepted 5 August 2023

To find a low temperature phase change material (PCM) that can be applied to the middle constant temperature chamber of the three chamber refrigerator, this study proposes a binary eutectic PCM of n-decanol and capric acid as a base liquid, expanded graphite as a support material, and boron nitride as a thermal conductivity enhanced particle to modify the material. The composite PCM with suitable phase change temperature and high phase change latent heat is prepared by the solution blending method. The leakage rate experiment determines the maximum adsorption ratio of expanded graphite to be 92 %. The chemical structure, microstructure and thermodynamic properties are characterized by Fourier transform infrared spectroscopy, differential scanning calorimetry, scanning electron microscopy, thermal conductivity analyzer and thermogravimetric analyzer. The results show that the n-decanol and capric acid binary eutectic PCM is fully wrapped in the porous structure of expanded graphite, and boron nitride thermal conductivity enhanced particles are well adsorbed on the surface and pores of expanded graphite. The n-decanol and capric acid phase change material, boron nitride thermal conductivity enhanced particles and expanded graphite support material are only physically combined and no chemical reaction occurred. The phase change temperature of CPCM-2 with 3 % boron nitride thermal conductivity enhanced particles is -3.68 °C, the phase change latent heat is 129.2 J/g, and the thermal conductivity is 0.75 W/m·K. It has good thermal stability and reliability in the application temperature range.
Keywords: the thermostatic chamber, phase change materials, boron nitride, thermal properties.

1. INTRODUCTION

With the development of science and technology and the continuous progress of society, the quality of life of people is becoming more and more desirable, and the requirements for food preservation are becoming more and more demanding. Applying phase change material (PCM) with good thermal properties in the refrigerator can effectively improve the refrigerator's performance and produce a more uniform temperature distribution. This is because the PCM can absorb heat at the appropriate phase change temperature, and then release the stored energy during the compressor shutdown stage, so that the preservation chamber can maintain a low temperature state for a longer period of time, thereby prolonging the preservation time of foods. It can be seen that phase change materials can resolve the contradiction between energy supply and demand in time and space, with high energy storage density and energy release processes close to a constant temperature. At present, the sustainable energy storage technology of PCMs [1] has carried out a lot of research in the fields of building energy conservation [2, 3], cold chain logistics [4 – 6], solar heat storage [7, 8] and so on, which has a wide application prospect. In the research of refrigerator cold storage technology, the operation cost and energy consumption of refrigerators are mainly reduced by peak load shifting and valley filling [9]. Under the background of peak-valley electricity price in many places [10], refrigerator cold storage technology can greatly reduce the waste of energy in low peak hours.

Scholars at home and abroad have carried out many studies on the application of energy storage methods for PCMs in the refrigeration field. The results show that the application of this method optimizes the energy storage devices of refrigerators, expands the temperature range of energy storage and improves the energy storage density. For example, Angelo et al. [11] used water as a PCM to place 15.6 kg of tap water on a bare tube evaporator through experimental research. It was shown that the introduction of the PCMs reduces the fluctuations of the product temperature during the operation of the refrigerator, reduces the temperature difference between the top and bottom of the refrigerator, and prolongs the closure time of the compressor and reduces the switching frequency. Abdolmaleki et al. [12] used polyethylene glycol (PEG) as a PCM and applied it to the refrigerator freezer. It was shown that the optimal mass and temperature of PEG were 2 kg and -20 °C, respectively. Compared with the routine refrigerator, a refrigerator freezer can reduce temperature fluctuations by 40.59 % and energy consumption by 8.37 %. Pirvaram et al. [13] used PEG-1000 and PEG-600 as PCMs in series and placed them on the back of an online tubular condenser. Experimental results showed that the compressor operating time was reduced, the temperature

* Corresponding author. Tel.: +86-18681692562.
E-mail: *410914219005@email.ncu.edu.cn* (P. Huang)

fluctuation inside the refrigerator was significantly reduced and the energy consumption was reduced by 13 % compared to the refrigerator with single PCMs or without PCMs. Sonnenrein et al. [14] used copolymer PCMs to apply them to the evaporator and condenser of the refrigerator. The results showed that the overall power consumption of the refrigerator was reduced by 17 % and the temperature fluctuation of the refrigerator was reduced from 4 °C to 0.5 °C. Guo et al. [15, 16] studied the effect of PCMs on the internal temperature fluctuation of the cold storage chamber through experiments, and placed the prepared low temperature PCMs in the air duct of the refrigerator cold storage chamber. The research results showed that the use of PCMs can reduce the temperature fluctuations in cold storage chambers and better preserve fresh vegetables, meat and other foods. Jonathan et al. [17] used commercial PCMs PLUSICE-10 and 19.5 wt.% NH_4Cl solution to improve the performance of household refrigerator evaporator. The results showed that the energy consumption of these two kinds of eutectic PCMs was reduced by 1.74 % and 5.81 % respectively, and the compressor operation time was reduced by 3.71 % and 9 % respectively. Gin et al. [18] placed a 10 mm thick PCM aluminum plate on the wall of the freezer, and the results showed that the temperature fluctuation in the freezer was significantly reduced and can still be maintained at a lower temperature in the event of power failure. In another study [19], it was found that the application of PCM in the freezer can reduce the energy consumption during the door opening by 7 % and the energy consumption during the defrosting by 8 % compared with the unused PCMs.

Currently, refrigerators on the market are not only double-door refrigerators in the traditional sense of refrigerators and freezers, but also triple-door refrigerators with constant temperature preservation chambers that allow fresh food and vegetable meat to have a longer shelf life. However, due to the short appearance time of refrigerators in the constant temperature preservation chamber, there are few reports on the application of PCMs to the refrigerator constant temperature chamber. Among the existing low temperature organic CPCMs, there are few studies on PCMs with phase change temperature around 0°C. Therefore, it is necessary to prepare a CPCM suitable for refrigerators on the basis of the existing refrigerator research, which has a phase change temperature of about 0°C, high latent heat of phase change, not easy to leak, no supercooling, no corrosion and low price. In this paper, n-decanol (DA) and capric acid (CA) are used as the base liquid, expanded graphite (EG) is used as the supporting material, and boron nitride (BN) is used as the thermally conductive particle to prepare the CPCM. The chemical structure, crystal structure, microstructure and thermodynamic properties of the CPCM are analyzed.

2. EXPERIMENTAL

2.1. Experimental materials and equipment

N-Decanol (DA) and capric acid (CA), analytically pure, purity > 98 %, produced by Aladdin Chemical Reagent Co., Ltd, (Shanghai, China). Expanded graphite (EG), 80 mesh, produced by Tengshengda Graphite Co., Ltd, (Shandong, China). Boron nitride (BN), purity > 99.9 %, particle size 1 – 2 μm, Aladdin Chemical Reagent Co., Ltd, (Shanghai, China). Anhydrous ethanol, analytical purity, purity > 99.7 %, produced by XiLong Technology Co., Ltd, (Guangdong China).

Vacuum drying oven (DZF-6210) from Shanghai Jinghong Experimental Equipment Co., Ltd, China. Constant temperature magnetic stirring water bath (HH-2J), from Lang Yue Instrument Manufacturing Co., Ltd, China. Constant temperature heating magnetic stirrer (DF-101s), from Zhengzhou Huate Instrument Co., Ltd, China. Electronic balance (FA1004N), from Shanghai Wante Electronics Co., Ltd, China. Fourier Transform Infrared Spectrometer (Nicolet 5700) from Thermoelectric Nicolet, USA. Differential Scanning Calorimeter (DSC 8500) from PE, USA. Thermogravimetric analyzer (TGA 4000) and scanning Electron Microscope (Quanta 200 FEG) from FEI, USA. And the thermal conductivity meter (TPS 2500s), from Compass Group, (Shenzhen, China).

2.2. Preparation of DA-CA base liquid

The cocrystal mass ratio of DA-CA is predicted to be 71.0:29.0 by the Schrader equation [20]. The DA and CA phase transition materials of a given mass were weighed in a 100 ml beaker at the theoretically predicted mass ratio. The constant temperature water bath is opened and the temperature of the water bath is adjusted to 40 ℃. After the temperature is constant, the mixed two-phase transition material is placed in a water bath at a constant temperature and placed in a magnetic stirrer rotor. The mixture was stirred with a magnetic stirrer at a rate of 300 r/min for 20 min to ensure that the DA and CA were sufficiently mixed. After stirring, the DA-CA binary eutectic phase transition material-based liquid is obtained by cooling to room temperature.

2.3. Preparation of DA-CA/EG

First, the optimal adsorption ratio of EG is determined. With the prepared DA-CA as the base solution, a 5 % – 10 % DA-CA/EG mixture is prepared with 5 % EG as the initial mass ratio and a 1 % mass ratio increment. First, weigh a certain mass of DA-CA/EG mixture into a 100 ml beaker, the magnetic stirrer water bath temperature is adjusted to 50 °C. When the temperature is stable, a certain mass of available EG is slowly poured into the beaker to be mechanically mixed according to the above proportions, for a mixing time of 60 min. After stirring, the DA-CA/EG is obtained by vacuum adsorption for 12 hours in a 70 °C vacuum drying oven. The preparation method of CPCMs with other mass ratios is the same as the above method. In the leakage rate experiment, a high-precision balance is used for the weighing. A filter paper is placed on the balance and zero, and then 0.5 g of the sample in the molten state was weighed and placed on the filter paper. After weighing, it is placed in a drying oven at 50 °C for static treatment. After half an hour, it is taken out and put into a new filter paper for weighing, and the quality at this time is recorded. The weighing mass of different DA-CA/EG ratios is obtained by weighing six times. According to the different leakage rates, DA-CA/EG with the best adsorption ratio can be obtained, and the next experiments are carried out with the best adsorption ratio.

2.4. Preparation of DA-CA/EG/BN

The beaker containing the prepared DA-CA base liquid is put into a magnetic stirring water bath, the temperature is set to 40 °C, put into the rotor, and the speed is set to 300 r/min. BN thermal conductivity enhanced particles are weighed according to mass ratios of 3 %, 5 %, 7 % and 9 %, and poured into a magnetically stirring water bath. The mixture is stirred at the same speed for 20 min under the action of magnetically stirring to fully mix with the DA-CA base solution. Anhydrous ethanol is chosen as the low boiling point solvent in the solution blending method. Anhydrous ethanol of a certain mass is weighed in a beaker according to the 1:3 mass ratio of DA-CA to anhydrous ethanol and slowly poured into the DA-CA/BN mixture. The addition of anhydrous ethanol dilutes the DA-CA/BN mixture, making it more diffuse. Finally, the mass ratio EG of the optimal adsorption rate obtained from the leakage rate experiment is introduced into the beaker of the above mixture. Most of the porous structure of EG is filled with anhydrous ethanol. The water bath temperature is adjusted to 60 °C. Under this temperature, anhydrous ethanol begins to evaporate slowly. With the evaporation of anhydrous ethanol, more DA-CA and BN particles start to enter the porous structure of EG. After 6 hours, most of the anhydrous ethanol has evaporated and the mixture in the beaker begins to become sticky. At this time, a mechanical stirrer is used to continue stirring. After 2 hours, the anhydrous ethanol is completely evaporated and DA-CA/EG/BN is obtained. Other BNs with different mass ratios adopt this same preparation process. Five CPCMs with different BN contents are named CPCM-1 (0% BN), CPCM-2 (3% BN), CPCM-3 (5% BN), CPCM-4 (7% BN) and CPCM-5 (9% BN).

3. RESULTS AND DISCUSSION

3.1. Determination of optimum adsorption ratio of EG

The addition of EG can prevent leakage and increase thermal conductivity, but it has little contribution to the latent heat of PCMs. The proportion of EG directly affects the thermal properties of the prepared CPCMs. The leakage rate experiment can determine the optimal adsorption ratio of EG. Table 1 shows the mass loss and the percentage of mass loss before and after the weighing.

Table 1. Mass loss after adding different mass ratios of EG

Sample	EG mass ratio, %	Before standing mass, g	After standing mass, g	Mass loss, g	Mass loss ratio, %
DA-CA/EG-5	5	0.5000	0.2972	0.2028	40.56
DA-CA/EG-6	6	0.5054	0.4224	0.0830	16.42
DA-CA/EG-7	7	0.5020	0.4257	0.0763	15.20
DA-CA/EG-8	8	0.5010	0.4908	0.0102	2.04
DA-CA/EG-9	9	0.5010	0.4836	0.0174	3.47
DA-CA/EG-10	10	0.5017	0.4833	0.0184	3.66

It can be seen from the table that with the increase of EG content, the leakage rate of DA-CA/EG gradually decreased. When the mass ratio of EG is 5 %, the leakage rate is as high as 40.56 %. This is because the content of DA-LA is too much beyond the adsorption capacity of EG, excessive molten PCM leaked out to be absorbed by filter paper. When the mass ratio of EG exceeds 8 %, the mass loss of the PCM is less than 4 %, which may be caused by measurement and observation errors. Among the materials prepared, CPCMs with a mass ratio of more than 8 % will not produce leakage but will affect the phase change latent heat. Therefore, based on the above results, the optimal mass ratio of EG in DA-CA is determined to be 8 %.

3.2. FT-IR analysis

Fig. 1 shows the FTIR spectra of EG, BN, DA-CA, CPCM-1 and CPCM-3. The absorption peak at 3421 cm^{-1} is the stretching vibration of the -OH functional group. The absorption peaks at 2959 cm^{-1}, 2925 cm^{-1} and 2854 cm^{-1} are the stretching vibrations of the C-H bond in -CH3 and -CH_2 groups, respectively. The absorption peak at 1714 cm^{-1} is a stretching vibration of the C=O bond in the -COOH functional group. The characteristic absorption peaks at 1466 cm^{-1} and 1378 cm^{-1} represent the shear bending vibration of the -CH_2 functional group and the in-plane bending vibration of the -CH_3 functional group. The characteristic absorption peak at 1056 cm^{-1} is an asymmetric stretching vibration of the -C-O functional group. The characteristic absorption peak at 721 cm^{-1} indicates the in-plane rocking vibration of the -CH_2 functional group. In the infrared spectrum of BN, a broad and sharp absorption peak near 1381 cm^{-1} represents the transverse optical stretching vibration of sp^2 -bonded h-BN [22], and the absorption peak near 791 cm^{-1} represents the transverse optical bending vibration of sp^2 -bonded h-BN [23]. EG is mainly composed of carbon elements and has no characteristic absorption peak in the Fourier infrared spectrum. In summary, it can be found that CPCM-1 and CPCM-3 have the same characteristic absorption peaks as DA-CA at 3421 cm^{-1}, 2959 cm^{-1}, 2925 cm^{-1}, 2854 cm^{-1}, 1714 cm^{-1}, 1466 cm^{-1}, 1378 cm^{-1}, 1056 cm^{-1} and 721 cm^{-1}, but the intensity of the absorption peaks has changed slightly, and no new absorption peaks have been generated. This indicates that the addition of EG and BN does not produce chemical changes, but rather physical compounding.

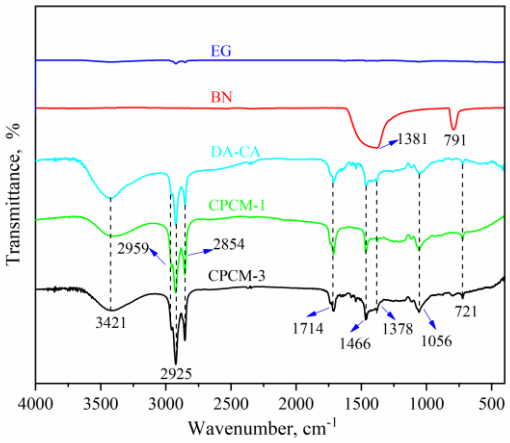

Fig. 1. Infrared spectra of EG, BN, DA-CA, CPCM-1 and CPCM-3

3.3. Morphological analysis

Fig. 2 is the SEM image of EG and CPCMs, where Fig. 2 a is the microstructure of EG, Fig. 2 b – f is the SEM image of CPCM-1 to CPCM-5. It can be seen from Fig. 2 a that EG has a porous structure, and its developed network pores can be clearly seen on the microscopic scale. This porous structure increases its specific surface area, and these pores are conducive to infiltrating into the molten PCM. Fig. 2 b shows that the pores of EG are adsorbed by DA-CA, and the outer pores are closed under the action of surface tension and capillary force to prevent the leakage of PCM. After the addition of the BN nanoparticles, the BN particles are uniformly dispersed on the surface and inside the pores of the EG, since the size of the BN particles is smaller than the size of the pores of the EG. It can be seen from Fig. 2 e that a large number of BN particles are attached to the surface of EG. On the one hand, it can be obtained that BN particles can be well combined with EG. On the other hand, it can be seen that BN nanoparticles with high thermal conductivity can effectively enhance the thermal conductivity of CPCMs.

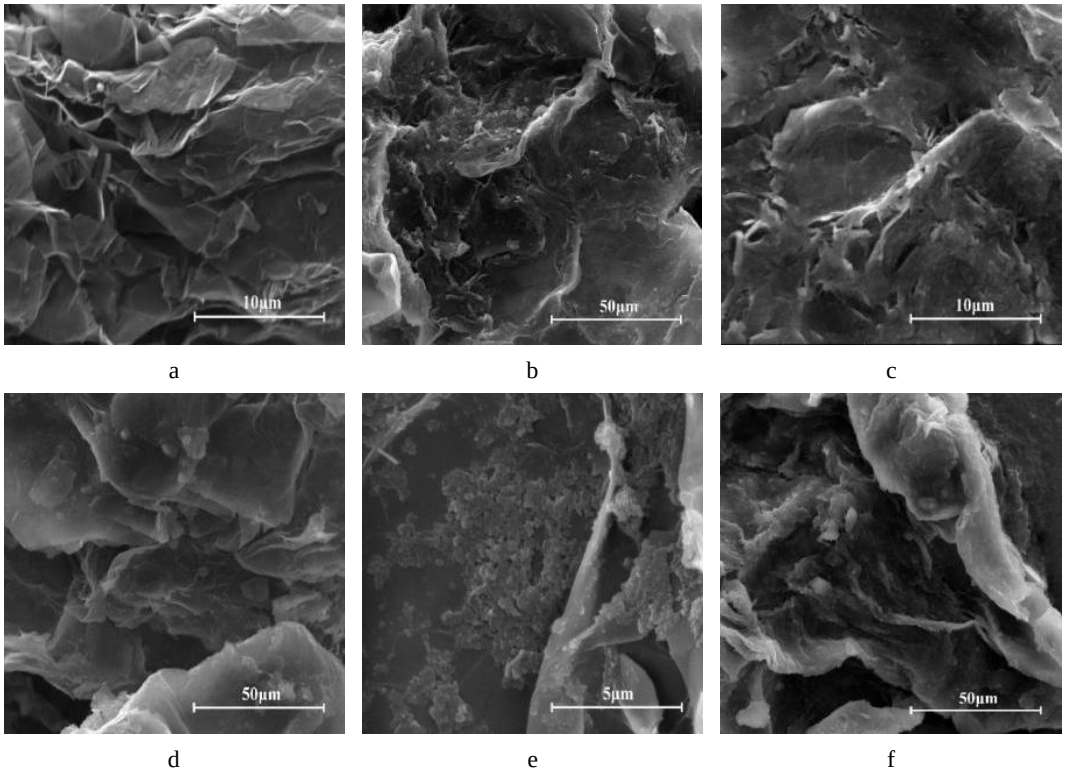

Fig. 2. SEM photographs: a – EG; b – CPCM-1; c – CPCM-2; d – CPCM-3; e – CPCM-4, f – CPCM-5

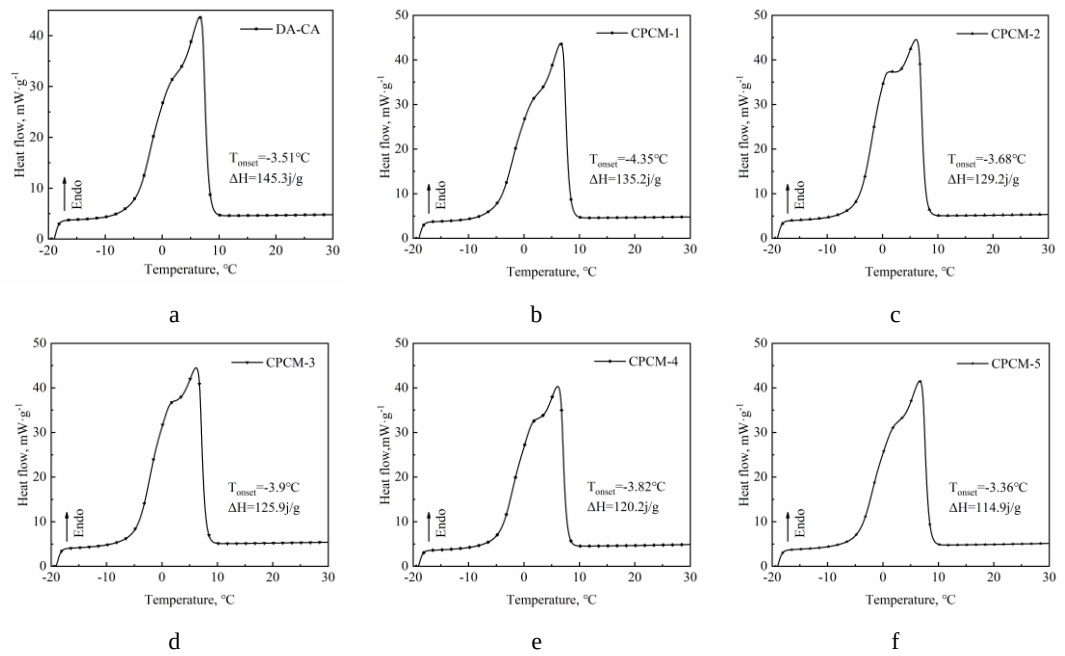

Fig. 3. a – DA-CA; b – CPCM-1; c – CPCM-2; d – CPCM-3; e – CPCM-4, f – CPCM-5 melting DSC curves

Table 2. DSC data of DA-CA and CPCMs samples

Sample	Initial temperature, ℃	Peak temperature, ℃	Latent heat of phase change, J/g
DA-CA	-3.51	6.32	145.3
CPCM-1	-4.35	6.63	135.2
CPCM-2	-3.68	6.1	129.2
CPCM-3	-3.9	6.19	125.9
CPCM-4	-3.82	6.11	120.2
CPCM-5	-2.36	6.65	114.9

3.4. DSC analysis

The phase change temperatures and enthalpies of DA-CA and CPCMs are shown in Fig. 3. The test temperature range is -20 °C to 30 °C, heating and cooling rate is 5 °C/min.

It can be seen from Table 2 that the phase change temperature of DA-CA is -3.51 °C and the latent heat of phase change is 145.3 J/g. The phase change temperatures of DA-CA, CPCM-1, CPCM-2, CPCM-3, CPCM-4 and CPCM-5 are -4.35 °C, -3.68 °C, -3.9 °C, -3.82 °C and-3.86 °C, respectively. Compared to DA-CA eutectic PCMs, the phase transition temperature of CPCMs is somewhat reduced to a certain extent, because the porous structure of EG limits the phase transition process of DA-CA. After adding EG and BN, the phase change temperature of CPCMs is consistent with that of pure DA-CA eutectic material, which indicates that the addition of EG and BN has no effect on the phase change temperature of DA-CA eutectic material. The phase change enthalpies of DA-CA, CPCM-1, CPCM-2, CPCM-3, CPCM-4 and CPCM-5 are 135.2 J/g, 129.2 J/g, 125.9 J/g, 120.2 J/g and 114.9 J/g, respectively. Obviously, the latent heat of CPCMs decreases with increasing BN mass fraction, because the latent heat in CPCMs is only related to the content of DA-CA. The percentages of decrease are 7.0 %, 11.1 %, 13.4 %, 17.3 % and 20.9 %, respectively. The proportion of its decline and the mass proportion of EG and BN added in DA-CA are high, which is mainly due to the error of DSC itself and the measurement error of electronic balance. Secondly, in the DSC measurement process, the ambient temperature is higher than the melting temperature of the CPCM. In the tableting process, the extrusion effect causes the DA-CA in the partially molten state of EG to leak under pressure, resulting in the DSC test quality of the PCM being lower than the weighing quality.

3.5. Thermal conductance analysis

As a ceramic material, BN has a similar structure and properties to graphite and has a high thermal conductivity, also known as white graphite [24]. Its thermal conductivity can reach 180 W/(m·K) [25]. BN also has some other important properties, such as high temperature resistance, thermal shock resistance, chemical inertness, non-toxicity and environmentally friendly [26]. Therefore, BN is selected as an effective thermal conductivity enhancement particle in this study. The thermal conductivity of DA-CA and CPCMs is measured using the Hot Disk method. Each sample material was carried out at a room temperature of 20 °C, and the results are shown in Fig. 4.

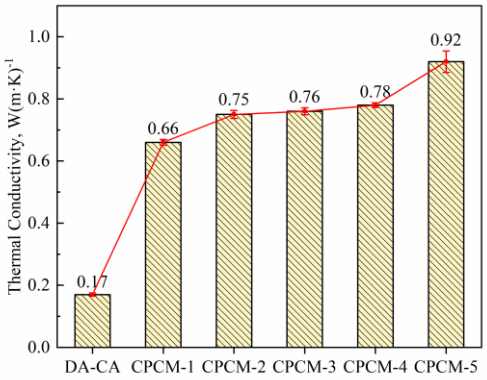

Fig. 4. Thermal conductivity of DA-CA and CPCM with different BN contents

The thermal conductivity of pure DA-CA is 0.17 W/(m·K). When 8 % EG is added, the thermal conductivity rapidly reaches 0.66 W/(m·K), which is 3.9 times that of pure DA-CA, which is attributed to the excellent thermal conductivity of the EG itself. To further increase the thermal conductivity of DA-CA, BN nanoparticles are added at ratios of 3 %, 5 %, 7 % and 9 %, respectively. When 3 % BN is added, the thermal conductivity is 0.75 W/(m·K), which is 13.6 % higher than that of DA-CA/EG, which is 4.41 times that of pure DA-CA. Fig. 4 shows that the thermal conductivity increases as the BN mass ratio increases. However, the effect of increasing the thermal conductivity is less pronounced compared to the case of compound phase transition materials added only with EG. This may be due to the addition of BN. When the amount is relatively low, it is in an unsaturated state in the CPCM, and the increase in thermal conductivity is not obvious [27]. With the increase of BN particles, thermal conductance path gradually increased, thermal conductivity begins to increase rapidly. When the mass ratio of BN is 9 %, the thermal conductivity of DA-CA/EG/BN is 0.92 W/(m·K), which is 5.41 times higher than that of pure DA-CA.

3.6. Thermogravimetric analysis

Fig. 5 shows the TGA degradation curves of DA-CA and CPCMs. Table 3 shows a mass loss after adding different mass ratios of EG. From Fig. 5 and Table 3, it can be seen that DA-CA and CPCMs are a single mass loss process between 20 °C and 500 °C, which is mainly the degradation of fatty alcohols and fatty acids in PCMs. The initial degradation temperature of DA-CA in the nitrogen atmosphere is 112.3 °C, and the maximum mass loss is 100 % when the temperature reaches 276.6 °C.

Table 3. Mass loss after adding different mass ratios of EG

Sample	Mass loss ratio of EG and BN, %	Starting temperature of decomposition, ℃	Maximum decomposition temperature, ℃	Residues, %
DA-CA	–	112.3	276.6	0.2
CPCM-1	8.0	115.4	270.7	9.4
CPCM-2	10.7	115.4	278.9	11.8
CPCM-3	12.4	115.4	261.8	13.9
CPCM-4	14.0	115.4	270.0	15.2
CPCM-5	15.6	115.4	275.2	17.5

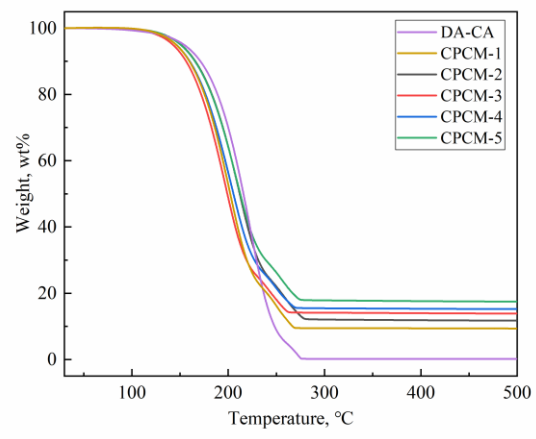

Fig. 5. TGA degradation curves of DA-CA and CPCMs

As the temperature continues to increase, the residual amount becomes 0. For CPCMs, the degradation temperature begins at 115.4 °C, 260 °C – 280 °C began to reach the maximum mass loss. The final residuals of CPCM-1, CPCM-2, CPCM-3, CPCM-4 and CPCM-5 are 9.4 %, 11.8 %, 13.9 %, 15.2 % and 17.5 %, respectively. The mass of these carbonized residues is essentially the same as that of the added EG and BN. It can also be seen from the figure that the initial degradation temperature of CPCMs is significantly higher than that of pure PCMs, which is because the Van Der Waals force between EG and PCMs increases the degradation temperature of PCMs. This also indicates that the addition of EG can effectively reduce the mass loss from the PCM, which improves the thermal stability of DA-CA.

4. CONCLUSIONS

In this work, a thermally enhanced DA-CA/EG/BN CPCM is prepared by solution blending method with DA-CA binary eutectic as PCM, EG as the support material and BN as the thermally enhanced particle. The chemical structure, microstructure and thermal properties have been studied experimentally. The conclusions are as follows:

1. Expanded graphite as a support material has good adsorption. The maximum adsorption ratio can be as high as 92 % by leakage rate experiments. At the same time, it has good thermal conductivity. Adding 8 % expanded graphite increases the thermal conductivity of DA-CA by a factor of 3.9.
2. The chemical structure and microstructure were characterized by FTIR and SEM. The results show that BN is well adsorbed on the surface and pores of EG, and that DA-CA, BN and EG are only physically bound in the absence of chemical reactions.
3. The thermal properties are characterized by DSC, TGA and thermal conductivity instruments. The results show that the phase transition temperature of CPCM-2 with 3 % BN is -3.68 °C, the latent heat is 129.2 J/g, and the thermal conductivity is 0.75 W/m·K, which is 4.4 times that of DA-CA/EG. Thermogravimetric analysis shows that it has good thermal stability and reliability in the application temperature range.

DA-CA/EG/BN composite PCM has a suitable phase transition temperature, good thermal stability, high latent heat and thermal conductivity, and is not prone to leakage. It has a good application prospect in the field of refrigerator preservation.

Acknowledgements

This research is supported by the Education Department of Jiangxi Province Science and Technology Research Project (191206).

REFERENCES

1. **Omara, A., Mohammedali, A.** Thermal Management and Performance Enhancement of Domestic Refrigerators and Freezers via Phase Change Materials *Innovative Food Science & Emerging Technologies* 66 2020: pp. 102522. https://doi.org/10.1016/j.ifset.2020.102522
2. **Li, B.** Application of Composite Phase Change Heat Storage Material in Building Energy Saving *Energy and Energy Saving* 01 2022: pp. 70 – 71. https://doi.org/10.16643/j.cnki.14-1360/td.2022.01.019
3. **Shu, Z., Zhong, K., Xiao, X, Jia, H., Lv, F., Chang, S.** Application Progress of Porous Nanomatrix Composite Phase Change Materials in Building Energy Saving *Chemical Progress* 40 (S2) 2021: pp. 265 – 278. https://doi.org/10.16085/j.issn.1000-6613.2021-0482
4. **Li, Y., Guo, Y., Fu, J.** Preparation and Thermal Properties of Binary Organic Phase Change Energy Storage Materials in Cold Chain Logistics *Journal of Composites* 39(06) 2022: pp. 1 – 15. https://doi.org/10.13801/j.cnki.fhclxb.20210721.002
5. **Song, Y., Zhang, N., Jing, Y., Cao, X., Yuan, Y.** Experimental and Numerical Investigation on Dodecane/Expanded Graphite Shape-stabilized Phase Change Material for Cold Energy Storage *Energy* 189 2019: pp. 116175. https://doi.org/10.1016/j.energy.2019.116175
6. **Zhang, S., Zhang, X., Xu, X., Zhao, Y.** Preparation and Properties of Decyl – Myristyl Alcohol/Expanded Graphite Low Temperature Composite Phase Change Material *Phase Transitions* 93 (5) 2020: pp. 491 – 503.

https://doi.org/10.1080/01411594.2020.1758319

7. **Ma, G., Liu, S., Xie, S., Jing, Y., Zhang, Q., Sun, J., Jia, Y.**Binary Eutectic Mixtures of Stearic Acid-n-butyramide/n-octanamide As Phase Change Materials for Low Temperature Solar Heat Storage *Applied Thermal Engineering* 111 2017: pp. 1052 – 1059. https://doi.org/10.1016/j.applthermaleng.2016.10.004
8. **Ye, Q.** Design, Preparation and Application of Solar Phase Change Heat Storage Composites *Shanghai: Shanghai Jiao Tong University Press* P.R. China, 2019. https://doi.org/10.27307/d.cnki.gsjtu.2019.003034
9. **Guo, L., Xue, G., Wu, C., Xie, Z., Liu, G., Bin, J.** Economic Benefit Analysis of Energy Storage System in Peak Shifting and Valley Filling *Power Demand Side Management* 21 (05) 2019: pp. 31 – 34. https://doi.org/10.3969/j.issn.1009-1831.2019.05.007
10. **Liu, M.** Consider the Impact of New Energy Consumption on Peak-valley tOU Electricity Price *Beijing: North China Electric Power University (Beijing) Press* P.R. China, 2021. https://doi.org/10.27140/d.cnki.ghbbu.2021.000804
11. **Maiorino, A., Del Duca, M.G., Mota-Babiloni, A., Greco, A., Aprea, C.** The Thermal Performances of a Refrigerator Incorporating A Phase Change Material *International Journal of Refrigeration* 100 2019: pp. 255 – 264. https://doi.org/10.1016/j.ijrefrig.2019.02.005
12. **Abdolmaleki, L., Sadrameli, S., Pirvaram, A.** Application of Environmental Friendly and Eutectic Phase Change Materials for The Efficiency Enhancement of Household Freezers *Renewable Energy* 145 2020: pp. 233 – 241. https://doi.org/10.1016/j.renene.2019.06.035
13. **Pirvaram, A., Sadrameli, S., Abdolmaleki, L.** Energy Management of a Household Refrigerator Using Eutectic Environmental Friendly PCMs in A Cascaded Condition *Energy Management* 181 2019: pp. 321 – 330. https://doi.org/10.1016/j.energy.2019.05.129
14. **Sonnenrein, G., Baumhögger, E., Elsner, A., Fieback, K., Morbach, A., Paul, A., Vrabec, J.** Copolymer-bound Phase Change Materials for Household Refrigerating Appliances: Experimental Investigation of Power Consumption, Temperature Distribution and Demand Side Management Potential *International Journal of Refrigeration* 60 2015: pp. 166 – 173. https://doi.org/10.1016/j.ijrefrig.2015.06.030
15. **Liu, Z., Guo, L., Li, A., Zhao, D.** Effect of Phase Change Material on The Temperature Fluctuation in The Freezer of Air-cooled Refrigerator *Journal of Beijing University of Technology* 43 (10) 2017: 1563 – 1568. https://doi.org/10.11936/bjutxb2016120024
16. **Guo, L., Liu, Z., Shi, H., Zhu, X., Li, M., Zhao, D.** Study on Temperature Fluction in Air-cooled Refrigerator with Phase Change Materials *Refrigeration and Air Conditioning* 31 (01) 2017: pp. 91 – 95. https://doi.org/10.3969/j.issn.1671-6612.2017.01.017
17. **Cofré-Toledo, J., Vasco, D.A., Isaza-Roldán, C.A., Tangarife, J.A.** Evaluation of An Integrated Household Refrigerator Evaporator with Two Eutectic Phase-change Materials *International Journal of Refrigeration* 93 2018: pp. 29 – 37. https://doi.org/10.1016/j.ijrefrig.2018.06.003
18. **Gin, B., Farid, M.** The Use of PCM Panels to Improve Storage Condition of Frozen Food *Journal of Food Engineering* 100 (2) 2010: pp. 372 – 376. https://doi.org/10.1016/j.jfoodeng.2010.04.016
19. **Gin, B., Farid, M., Bansal, P.** Effect of Door Opening and Defrost Cycle on A Freezer with Phase Change Panels *Energy Conversion and Management* 51 (12) 2010: pp. 2698 – 2706. https://doi.org/10.1016/j.enconman.2010.06.005
20. **Chen, Y., Liu, Y., Wang, Z.** Preparation and Characteristics of Microencapsulated Lauric Acid as Composite Thermal Energy Storage Materials *Materials Science (Medžiagotyra)* 26 (1) 2019: pp. 88 – 93. https://doi.org/10.5755/j01.ms.26.1.21303
21. **Yang, X., Yuan, Y., Zhang, N., Cao, X., Liu, C.** Preparation and Properties of Myristic–palmitic–stearic Acid/Expanded Graphite Composites as Phase Change Materials for Energy Storage *Solar Energy* 99 2014: pp. 259 – 266. https://doi.org/10.1016/j.solener.2013.11.021
22. **Mirkarimi, P., Mccarty, K., Medlin, D.** Review of Advances in Cubic Boron Nitride Film Synthesis *Materials Science and Engineering: R: Reports* 21 (2) 1997: pp. 47 – 100. https://doi.org/10.1016/S0927-796X(97)00009-0
23. **Djouadi, M.** Deposition of Boron Nitride Films by PVD Methods: Transition from h-BN to c-BN *Surface and Coatings Technology* 180-181 2004: pp. 174 – 177. https://doi.org/10.1016/j.surfcoat.2003.10.156
24. **Jeong, S.G., Lee, J.H., Seo, J., Kim, S.** Thermal Performance Evaluation of Bio-based Shape Stabilized PCM with Boron Nitride for Energy Saving *International Journal of Heat and Mass Transfer* 71 2014: pp. 245 – 250. https://doi.org/10.1016/j.ijheatmasstransfer.2013.12.017
25. **Yang, J., Wang, C., Zhou, S., Zhen, M., Ye, H.** Preparation and Properties of Polyethylene / Graphene / Boron Nitride Thermal Conductive Composite *Chemical Technology and Development* 51 (Z1) 2022: pp. 15 – 19. https://doi.org/10.3969/j.issn.1671-9905.2022.01.004
26. **Eichler, J., Lesniak, C.** Boron Nitride (BN) and BN Composites for High-temperature Applications *Journal of the European Ceramic Society* 28 (5) 2008: pp. 1105 – 1109. https://doi.org/10.1016/j.jeurceramsoc.2007.09.005
27. **Zhang, K., Tao, P., Zhang, Y., Liao, X., Nie, S.** Highly Thermal Conductivity of CNF/AlN Hybrid Films for Thermal Management of Flexible Energy Storage Devices *Carbohydrate Polymers* 213 2019: pp. 228 – 235 https://doi.org/10.1016/j.carbpol.2019.02.087